Soft X-ray emission during the deep solar minimum of 2009

Marek Stęślicki[1], Szymon Gburek[1], Janusz Sylwester[1], Barbara Sylwester[1], Marek Siarkowski[1], Magdalena Gryciuk[1] Tomasz Mrozek[1,2]

[1]Space Research Centre Polish Academy of Sciences, Solar Physics Division, Poland
[2]Astronomical Institute, University of Wrocław, Poland

SphinX: Solar Photometer in X-rays

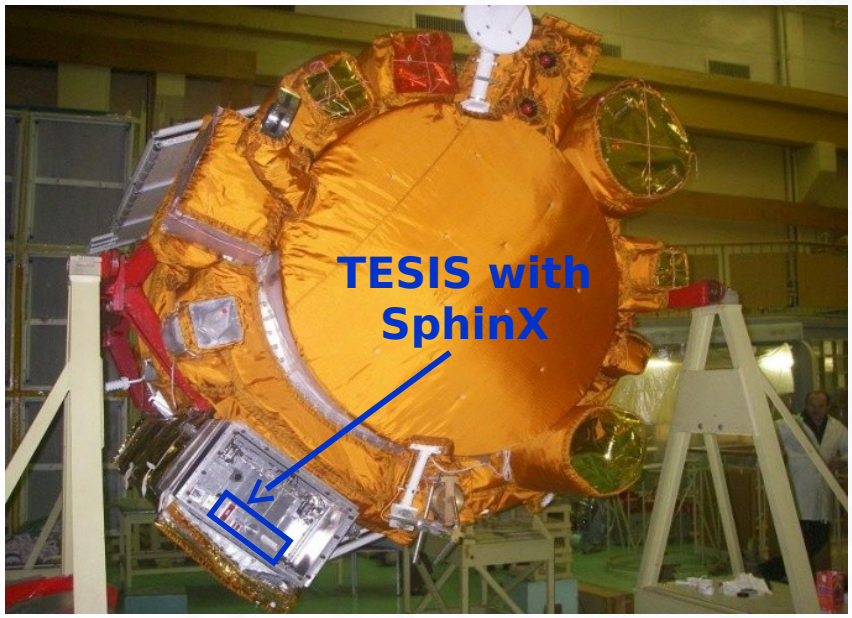

- SphinX flew on the Russian CORONAS–PHOTON satellite.
  It was the third satellite launched in the *Russian Complex Orbital Observations Near-Earth of Activity of the Sun* (CORONAS) program.
- SphinX operated in orbit within the TESIS EUV and X telescope assembly developed at the P.N. Lebedev Physical Institute (LPI).
- The spacecraft was launched on 30 January 2009 at 13:30 UT from the Plesetsk Cosmodrome in northern Russia.

Basic characteristics

Mass 3.7 kg

Power 10 W

Telemetry – 150MB a day

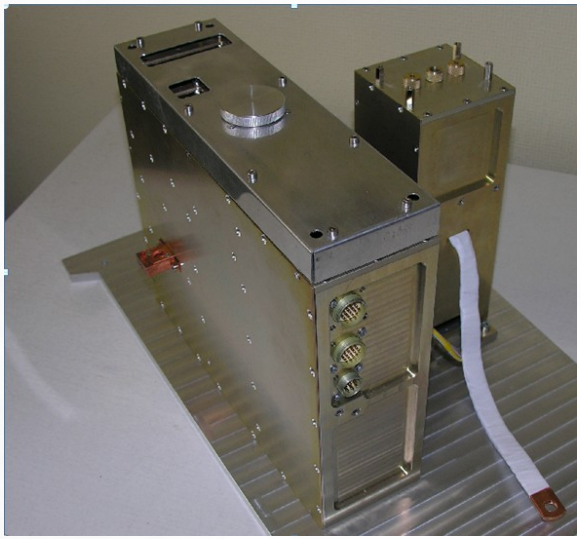

The spacecraft orbit was circular with **an inclination angle of 82.5°**, initial height 550 km, and **period of 95 minutes**.

The **accuracy** of the spacecraft orientation with respect to the Sun was better than **three arcminutes** after stabilization.

Monitoring of solar soft X-ray flux in the energy range **≈1.0–15.0 keV**

SphinX Detectors

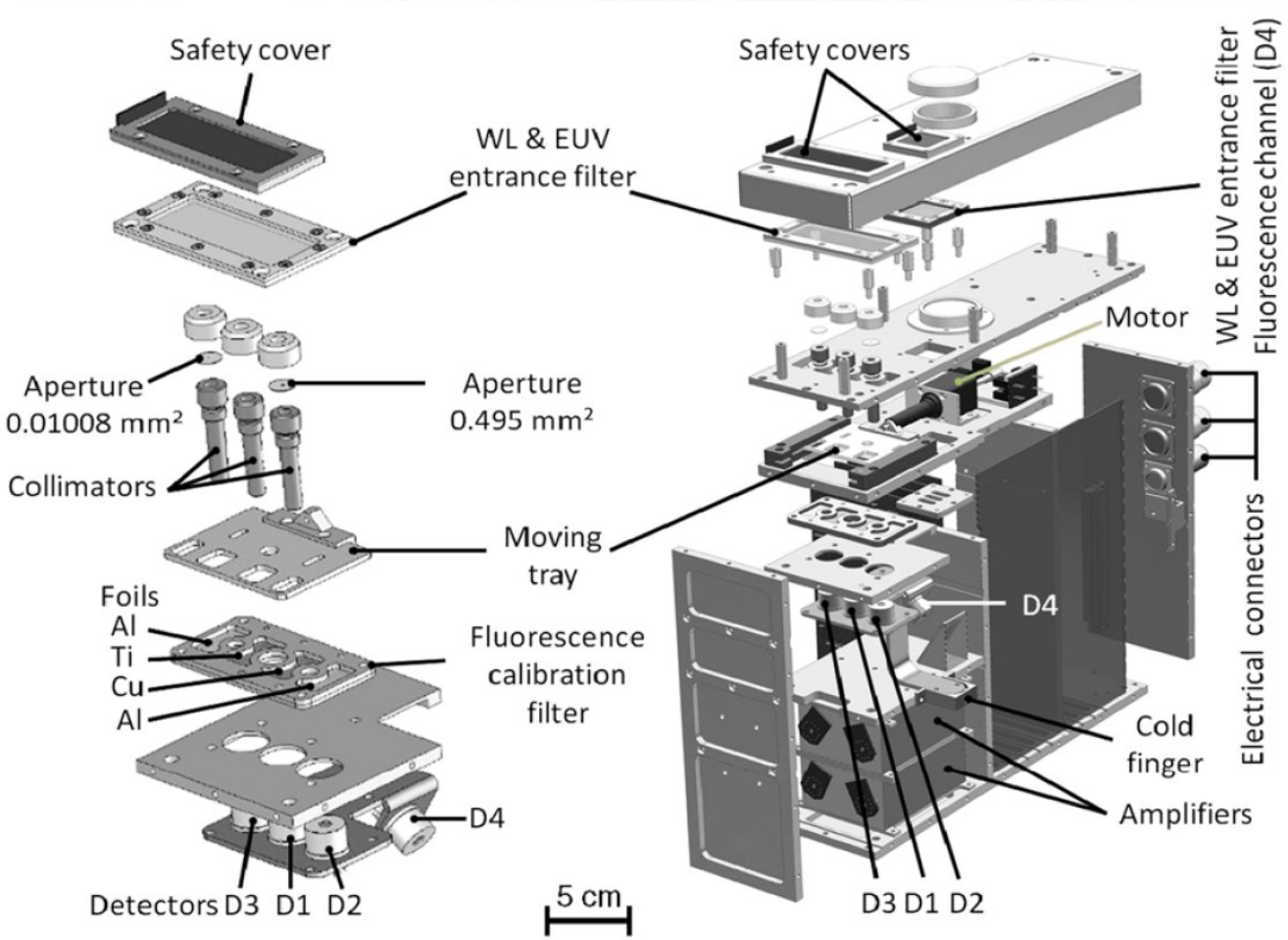

SphinX CAD exploded plots. The X-ray optical bench of the instrument is shown in more detail at the left.

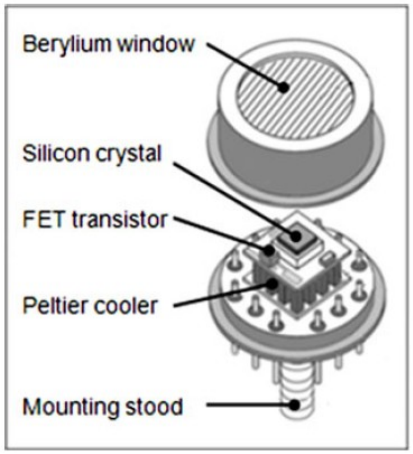

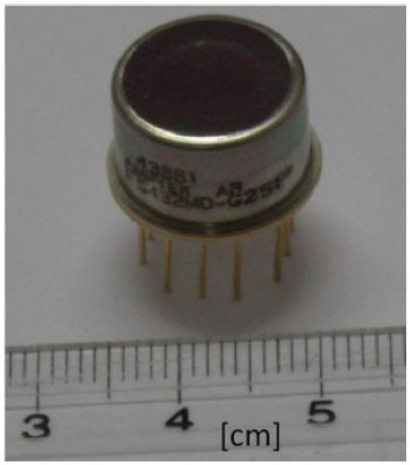

Amptek XR-100CR
detector used in SphinX.

Three PIN-diode detectors

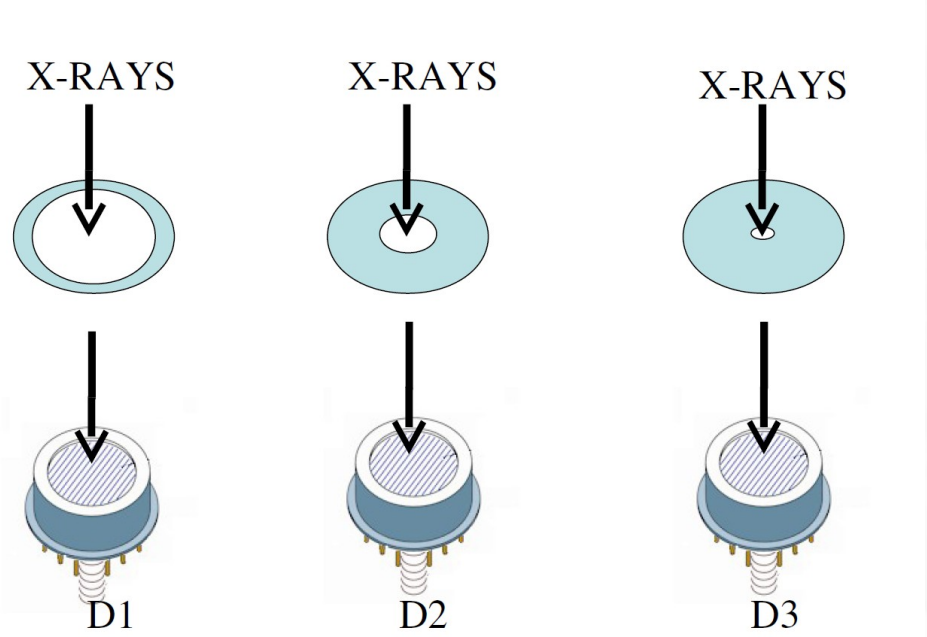

Three PIN-diode detectors with decreasing appertures are used to cover 7 orders of variability of solar X-ray flux magnitude.

X-ray flux level	Low	Moderate	High	High
Detector Name	D1	D2	D3	D4
Observation type	Direct Solar X-rays	Direct Solar X-rays	Direct Solar X-rays	Fluorescence
Aperture [mm^2]	21.500^{A}	0.4947^{S}	0.01008^{S}	11.1^{A}
Energy FWHM [eV]	480^{B}	350^{B}	370^{B}	290^{P}
Pulse width [μs]	1.25^{E}	4.17^{E}	4.17^{E}	4.17^{E}
Energy range [keV]	1.0 – 15	0.85 – 15	0.85 – 15	0.85 – 15

Orbital background

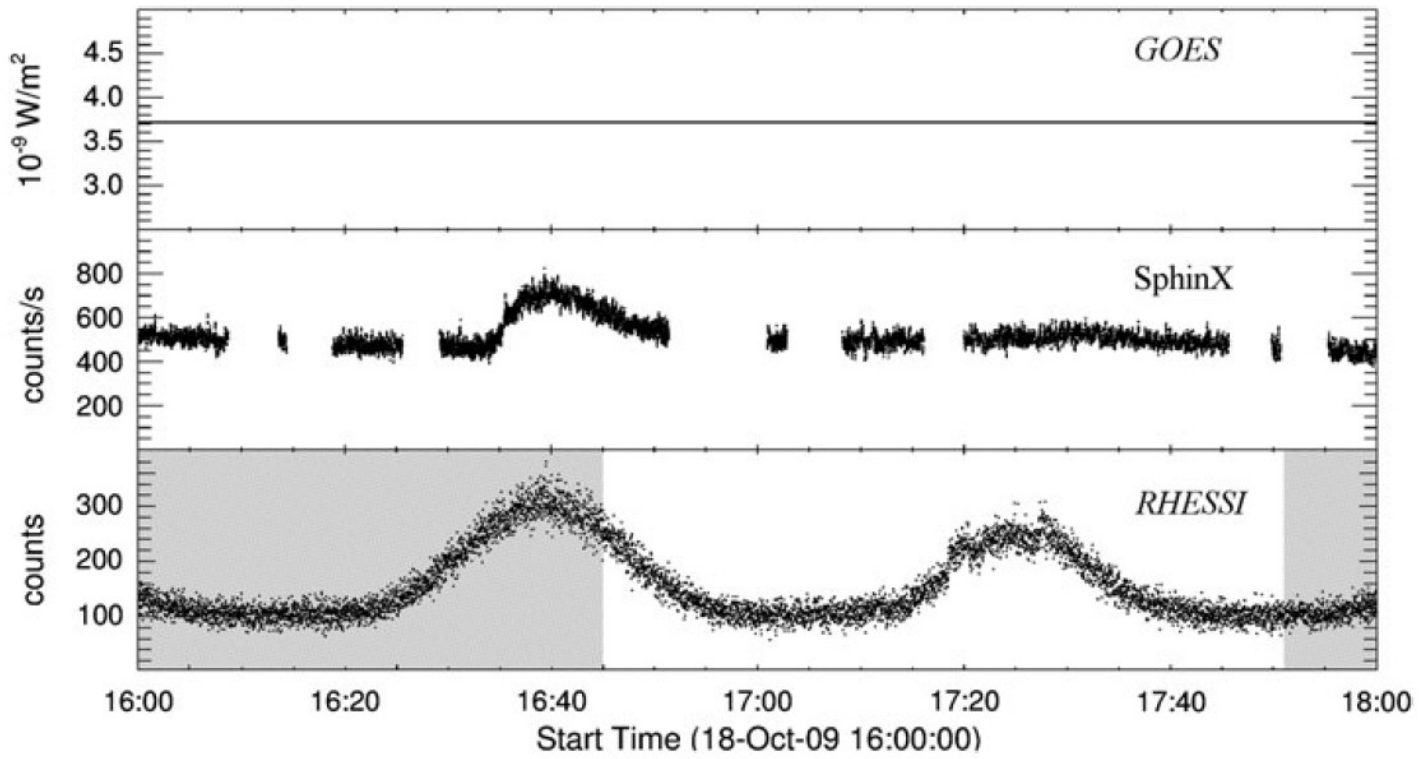

Figure 1 Comparison of solar X-ray observations on 18 October 2009. Top: the GOES light curve in 1 – 8 Å (1.5 – 12.4 keV) channel; SphinX light curve in the same energy range as for GOES is plotted in the middle panel. The RHESSI light curve in (3.0 – 12.4 keV) range is shown at the bottom. Shaded areas in this plot are for intervals of time when RHESSI was eclipsed. The GOES curve is entirely flat and follows the instrument sensitivity threshold, 3.7×10^{-9} W m^{-2}. Substantial modulation from the orbital background is seen in the RHESSI light curve. Due to the satellite night, the RHESSI also missed a small flaring event, which is seen in the SphinX light curve.

Gburek et al., 2013, SoPh 283, 631

Orbit Environment

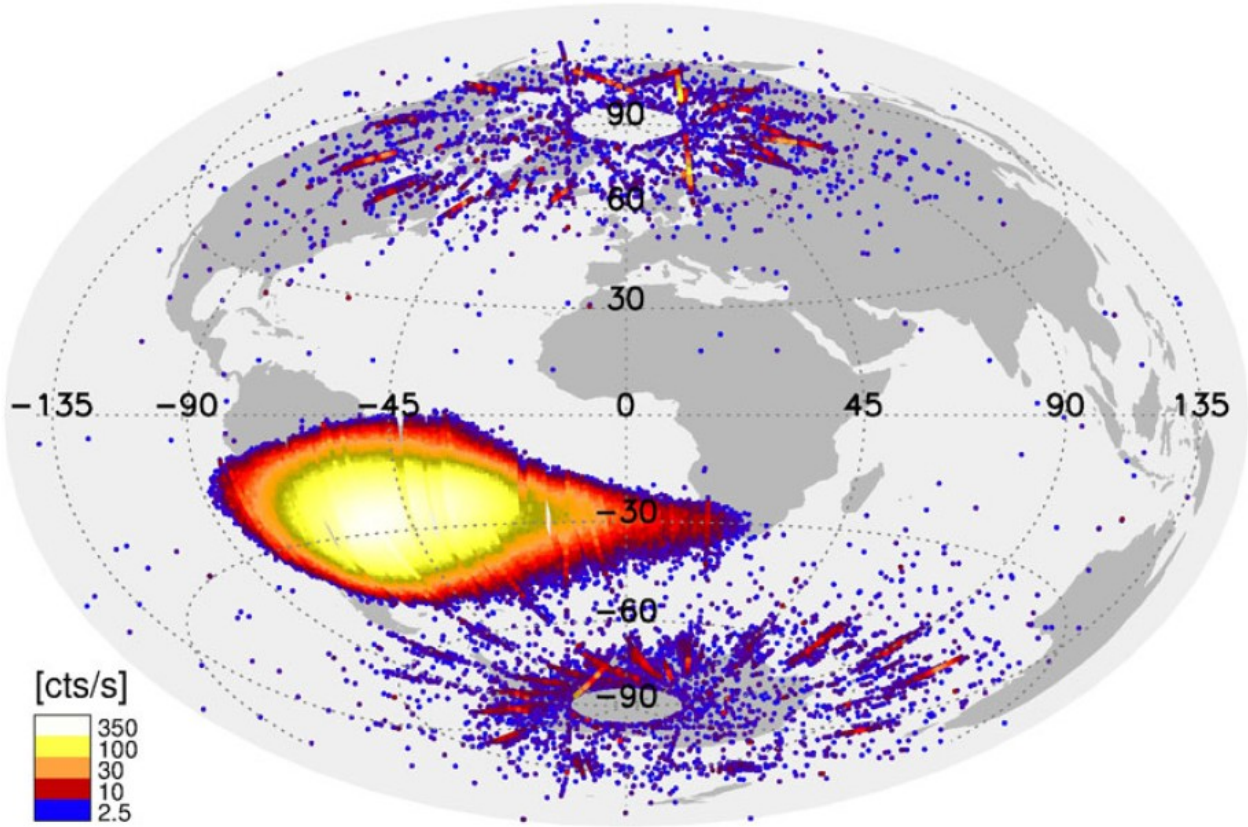

Figure 4 Energetic-particle distribution over CORONAS–PHOTON orbit as observed by SphinX. It is seen that particles contribute to measurement everywhere on the orbit. This contribution is small in equatorial regions. It increases substantially in radiation belts and becomes particularly strong in the SAA area.

Gburek et al., 2013, SoPh 283, 631

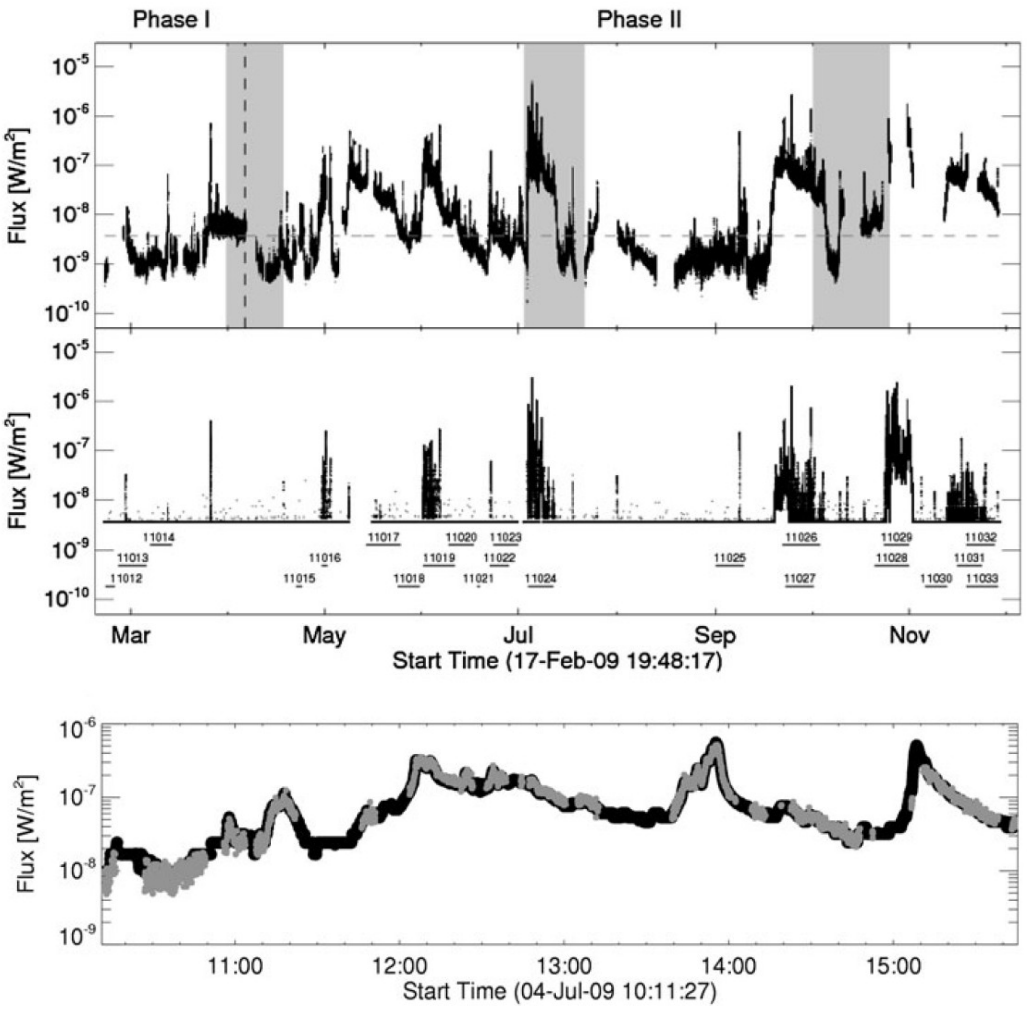

SphinX observed the Sun in soft X-rays during a period of a very low solar activity between Cycle 23 and 24 and in the Cycle 24 early rise phase.

January 30 – November 29, 2009

Figure 2 The SphinX light curve over the mission duration is shown in the upper panel. The black dashed vertical line is for 6 April 2009, when the first mission phase ended and the second began. The horizontal gray dashed line shows the GOES sensitivity detection threshold (3.7×10^{-9} W m^{-2}). Gray vertical strips show the time intervals when satellite nights did not occur – the long spacecraft days. The GOES light curve is shown in the middle panel for comparison. Active-region lifetimes are indicated by gray intervals there. Numbers of the active regions as attributed by the National Oceanic and Atmospheric Administration (NOAA) are given above. The bottom panel shows a comparison of SphinX (gray curve) and GOES (black curve) fluxes in the 1 – 8 Å wavelength range for a shorter time period. Gaps in SphinX data occur for temporal intervals when the detectors were exposed to energetic particles.

Gburek et al., 2013, SoPh 283, 631

SphinX D1 – GOES 1-8 Å

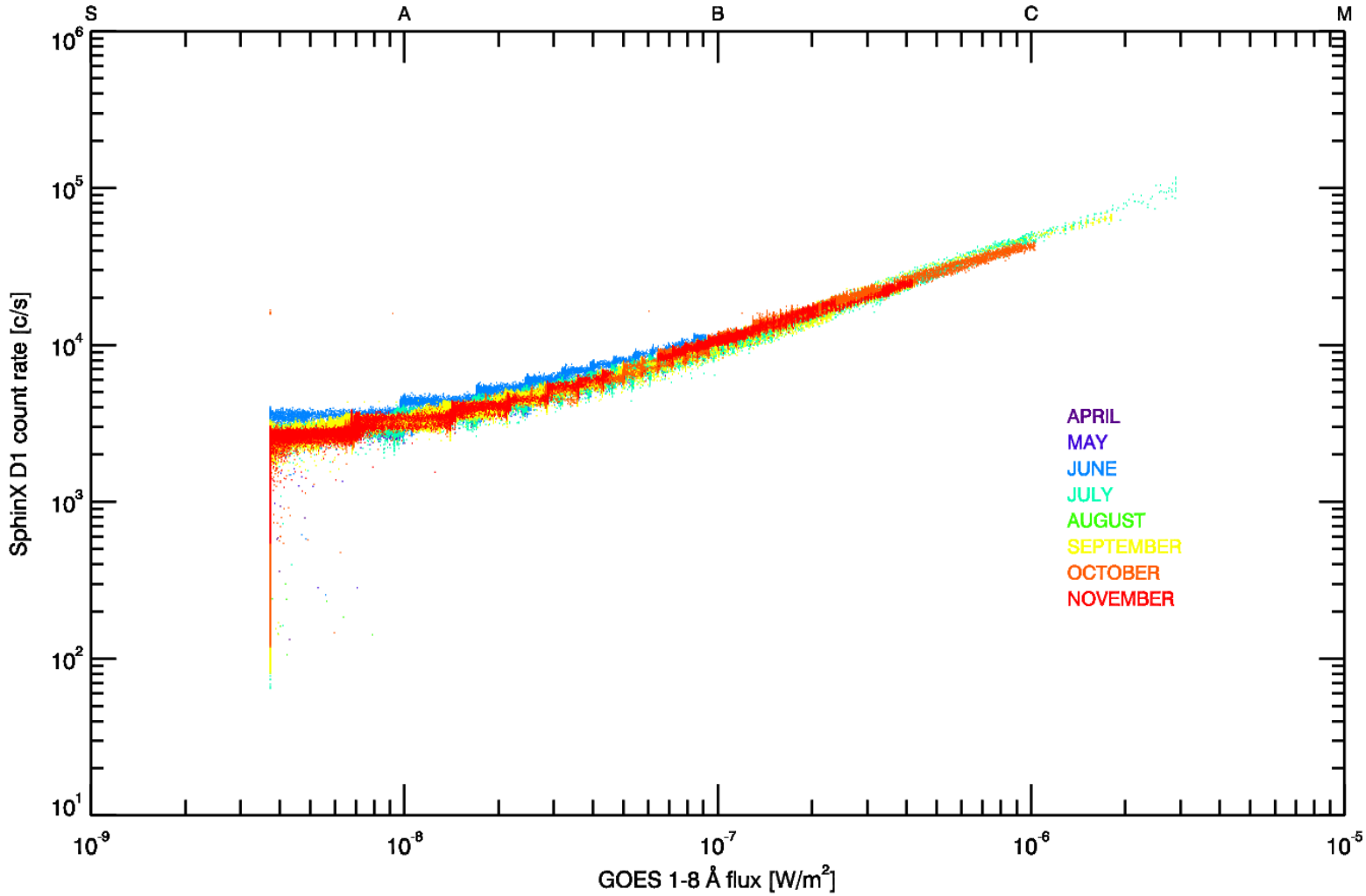

SphinX D1 – XRT Ti/Poly

(1 keV – 15 keV) (0.7 keV – 2.3 keV)

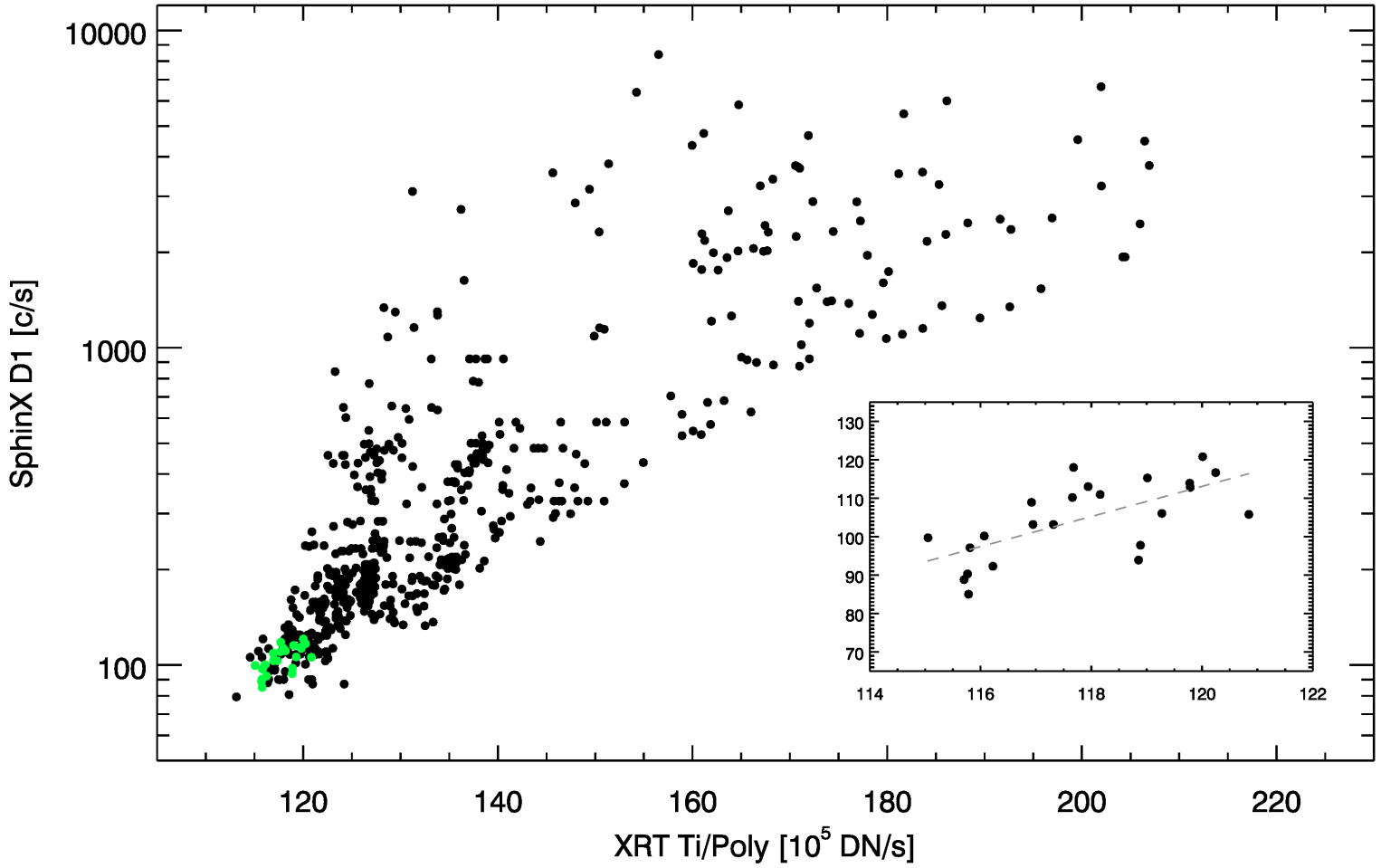

Evolution of AR 11017 observed by SphinX

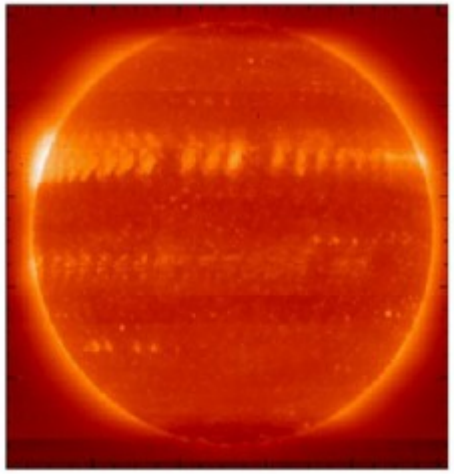

Composite image (76 images superimposed) from the XRT telescope is given.

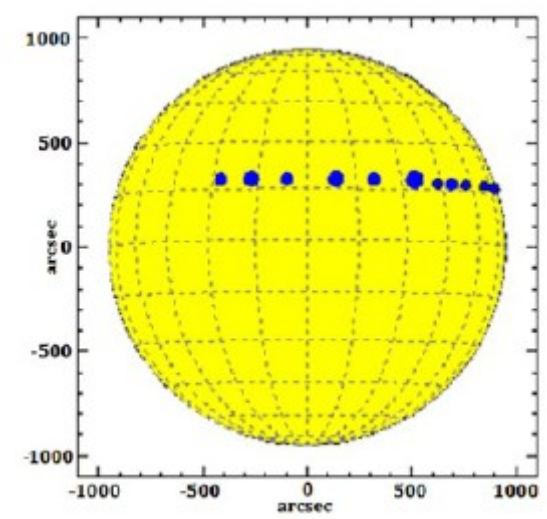

The daily positions of AR 11017 indicated by dark circles. The circle diameter is proportional to the logarithm of the AR area. Positions and sizes were taken from NOAA AR reports

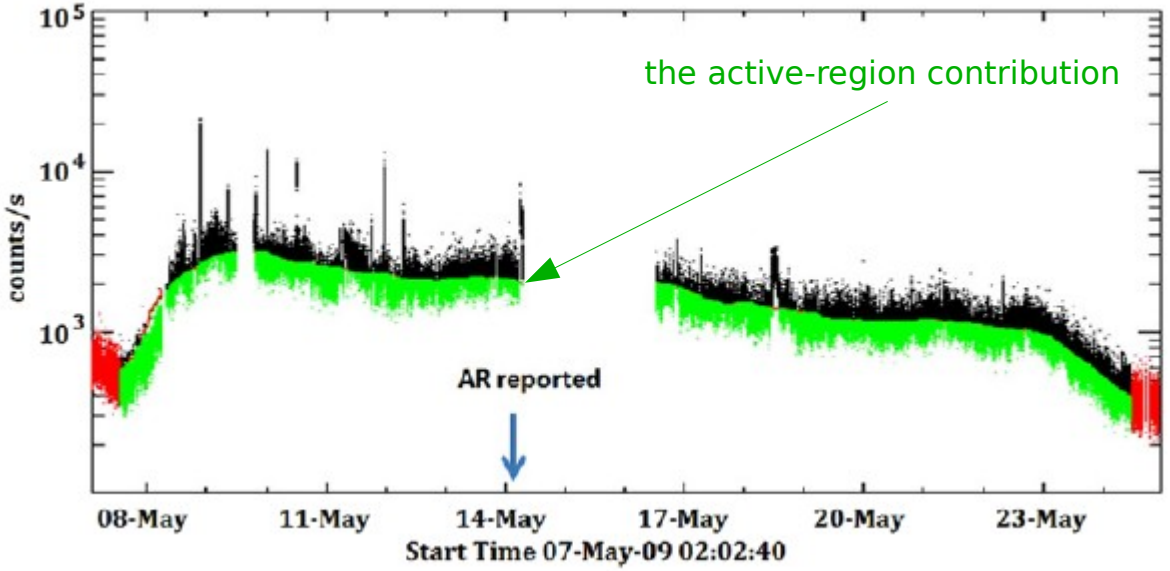

Evolution of Active Region 11017 as seen in SphinX data

Periods of especially low activity

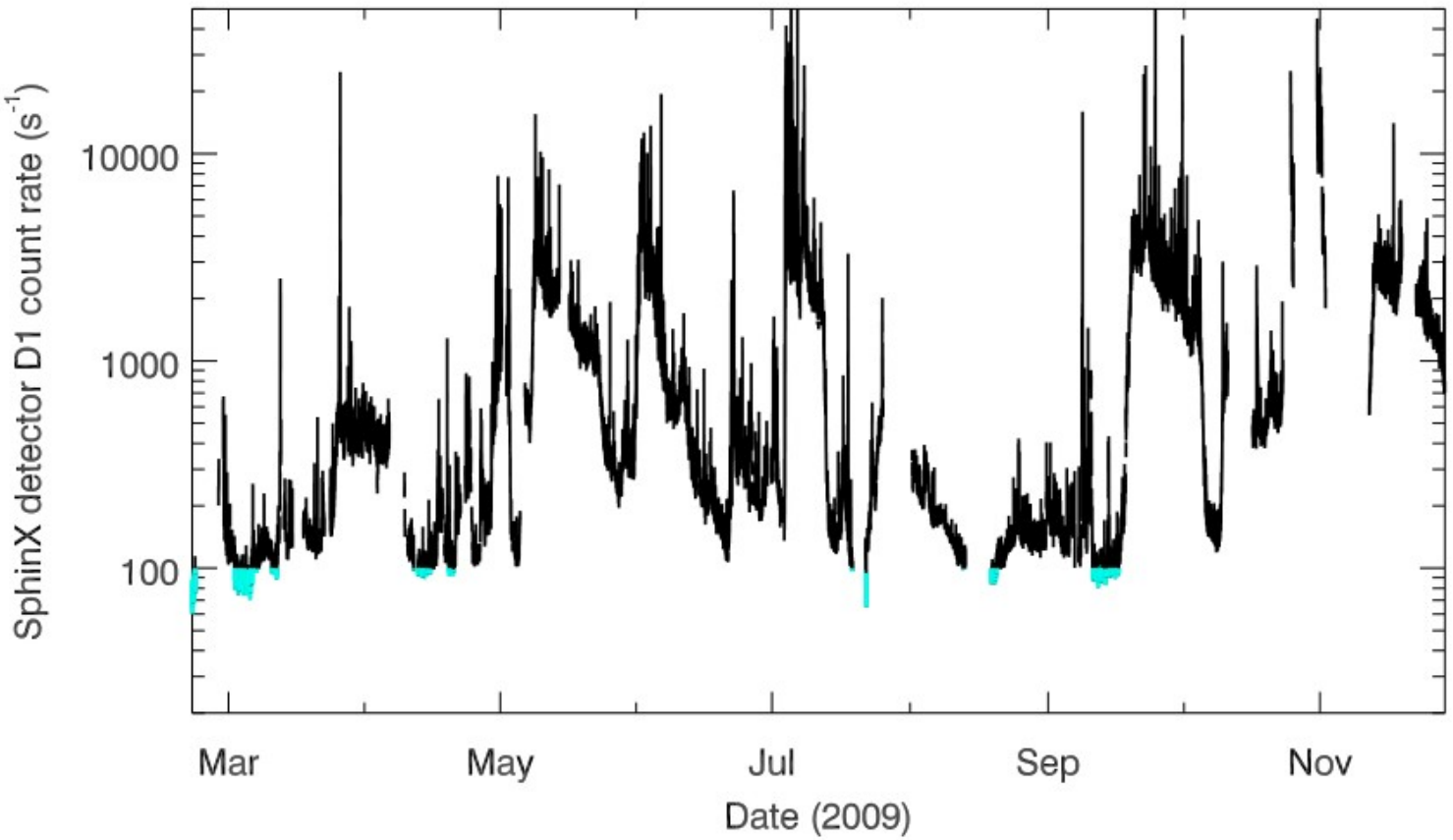

Figure 1. X-ray emission as recorded by the SphinX D1 detector (in counts s^{-1}), from daily averages over the period 2009 February 20–November 28. Portions of the curve marked gray (blue in the online journal) show periods selected for especially low activity. The detector count rates are as observed, i.e., not corrected for the slight variation in the Earth–Sun distance.

Intervals of Very Low Activity

SphinX Measurements During Intervals of Very Low Activity in 2009

Interval	Time Range (Dates are 2009)	T_e (MK)[a]	$\log_{10}$ EM[a] (EM in cm^{-3})	SphinX X-ray (1–8 Å) Flux ($W\ m^{-2}$)[b]	1–15 keV Luminosity ($erg\ s^{-1}$)[b]
1	Feb 20 20:12–Feb 21 05:46	1.73 (.04)	47.81 (.01)	4.91 (−10)	4.63 (22)
2	Feb 21 06:33–Feb 21 15:21	1.81 (.04)	47.72 (.01)	6.62 (−10)	5.10 (22)
3	Mar 2 12:23–Mar 2 17:57	1.89 (.04)	47.61 (.01)	7.70 (−10)	5.15 (22)
4	Mar 3 06:02–Mar 4 00:15	1.88 (.05)	47.62 (.01)	7.60 (−10)	5.15 (22)
5	Mar 4 09:05–Mar 4 17:49	1.84 (.04)	47.68 (.01)	7.21 (−10)	5.22 (22)
6	Mar 4 23:21–Mar 5 11:21	1.79 (.03)	47.78 (.01)	6.48 (−10)	5.33 (22)
7	Mar 5 18:42–Mar 5 20:56	1.80 (.05)	47.69 (.01)	5.90 (−10)	4.66 (22)
8	Mar 11 15:02–Mar 11 20:34	1.79 (.04)	47.83 (.01)	7.35 (−10)	6.03 (22)
9	Apr 12 13:05–Apr 12 17:30	1.74 (.03)	47.93 (.01)	6.68 (−10)	6.16 (22)
10	Apr 13 15:50–Apr 13 20:12	1.72 (.02)	47.95 (.01)	6.38 (−10)	6.11 (22)
11	Apr 14 05:33–Apr 14 11:19	1.74 (.03)	47.92 (.01)	6.66 (−10)	6.10 (22)
12	Apr 19 10:31–Apr 19 14:22	1.85 (.03)	47.75 (.01)	8.64 (−10)	6.16 (22)
13	Apr 19 20:11–Apr 20 05:19	1.92 (.03)	47.64 (.01)	9.85 (−10)	6.20 (22)
14	Apr 20 06:09–Apr 20 12:59	1.88 (.02)	47.73 (.01)	9.76 (−10)	6.56 (22)
15	Jul 18 14:13–Jul 18 16:54	1.72 (.03)	48.01 (.01)	7.28 (−10)	7.01 (22)
16	Jul 18 18:30–Jul 19 02:09	1.73 (.03)	48.00 (.01)	7.59 (−10)	7.09 (22)
17	Jul 22 00:52–Jul 22 04:13	1.75 (.03)	47.97 (.01)	8.17 (−10)	7.31 (22)
18	Aug 12 19:14–Aug 13 09:36	1.74 (.03)	47.98 (.01)	7.79 (−10)	7.11 (22)
19	Aug 19 05:39–Aug 19 20:01	1.72 (.03)	47.96 (.01)	6.34 (−10)	6.14 (22)
20	Aug 19 23:11–Aug 20 10:43	1.68 (.03)	48.05 (.01)	5.99 (−10)	6.44 (22)
21	Aug 20 12:00–Aug 20 18:40	1.87 (.04)	47.75 (.01)	9.89 (−10)	6.81 (22)
22	Sep 11 09:30–Sep 11 22:12	1.79 (.04)	47.83 (.01)	7.64 (−10)	6.16 (22)
23	Sep 11 22:54–Sep 12 12:37	1.70 (.03)	47.99 (.01)	6.05 (−10)	6.12 (22)
24	Sep 13 02:17–Sep 13 07:46	1.69 (.03)	48.01 (.01)	6.10 (−10)	6.27 (22)
25	Sep 13 19:33–Sep 13 21:11	1.68 (.06)	48.02 (.02)	5.80 (−10)	6.13 (22)
26	Sep 14 21:04–Sep 15 07:37	1.79 (.03)	47.84 (.01)	7.79 (−10)	6.28 (22)
27	Sep 16 01:50–Sep 16 07:34	1.71 (.02)	47.99 (.09)	6.53 (−10)	6.48 (22)

Sylwester et al., 2012, ApJ 751, 111

Intervals of Very Low Activity

SphinX Measurements During Intervals of Very Low Activity in 2009

Interval	Time Range (Dates are 2009)	T_e (MK)[a]	$\log_{10}$ EM[a] (EM in cm^{-3})	SphinX X-ray (1–8 Å) Flux ($W\ m^{-2}$)[b]	1–15 keV Luminosity ($erg\ s^{-1}$)[b]
1	Feb 20 20:12–Feb 21 05:46	1.73 (.04)	47.81 (.01)	4.91 (−10)	4.63 (22)
2	Feb 21 06:33–Feb 21 15:21	1.81 (.04)	47.72 (.01)	6.62 (−10)	5.10 (22)
3	Mar 2 12:23–Mar 2 17:57	1.89 (.04)	47.61 (.01)	7.70 (−10)	5.15 (22)
4	Mar 3 06:02–Mar 4 00:15	1.88 (.05)	47.62 (.01)	7.60 (−10)	5.15 (22)
5					(22)
6					(22)
7					(22)
8					(22)
9					(22)
10					(22)
11					(22)
12					(22)
13					(22)
14					(22)
15					(22)
16					(22)
17					(22)
18					(22)
19					(22)
20	Aug 19 23:11–Aug 20 10:43	1.68 (.03)	48.05 (.01)	5.99 (−10)	6.44 (22)
21	Aug 20 12:00–Aug 20 18:40	1.87 (.04)	47.75 (.01)	9.89 (−10)	6.81 (22)
22	Sep 11 09:30–Sep 11 22:12	1.79 (.04)	47.83 (.01)	7.64 (−10)	6.16 (22)
23	Sep 11 22:54–Sep 12 12:37	1.70 (.03)	47.99 (.01)	6.05 (−10)	6.12 (22)
24	Sep 13 02:17–Sep 13 07:46	1.69 (.03)	48.01 (.01)	6.10 (−10)	6.27 (22)
25	Sep 13 19:33–Sep 13 21:11	1.68 (.06)	48.02 (.02)	5.80 (−10)	6.13 (22)
26	Sep 14 21:04–Sep 15 07:37	1.79 (.03)	47.84 (.01)	7.79 (−10)	6.28 (22)
27	Sep 16 01:50–Sep 16 07:34	1.71 (.02)	47.99 (.09)	6.53 (−10)	6.48 (22)

Temperature: **1.78 ± 0.07 MK**

Logarithm of emission measure: **47.85 ± 0.14 cm^{-3}**

X-ray flux (1-8Å): **$7.21\times10^{-10} \pm 1.26\times10^{-10}$ Wm^{-3}**

1-15 keV X-ray luminosity: **$6.07\times10^{22} \pm 0.73\times10^{22}$ erg s^{-1}**

Sylwester et al., 2012, ApJ 751, 111

Spectra of Quiet Sun

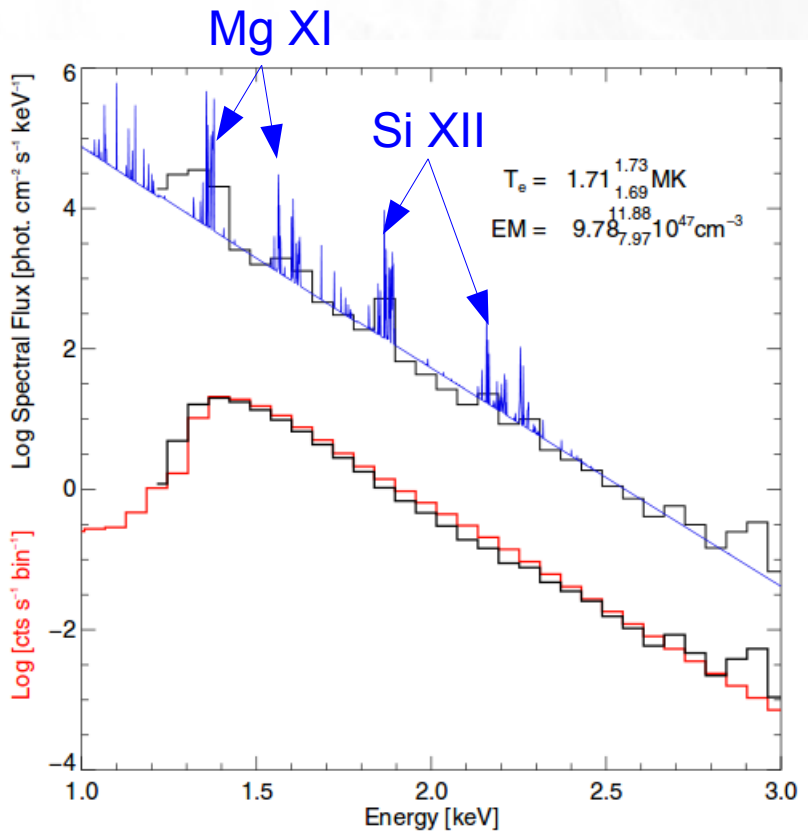

Figure 2. Averaged photon spectrum in the 1–3 keV range (upper histogram) over a time period on 2009 September 16 between 01:50 UT and 07:33 UT, made up of intervals when the total SphinX D1 count rate was below 110 counts s^{-1}. The energy bins correspond to those in the count rate spectrum (lower histograms). The blue curve is the CHIANTI photon spectrum at a few eV resolution showing principal line groups. In the count rate spectra, the black histogram is the observed SphinX spectrum, and the red histogram shows the best fit to the count rate spectrum with estimated temperature and emission measure indicated in the legend.

Sylwester et al., 2012, ApJ 751, 111

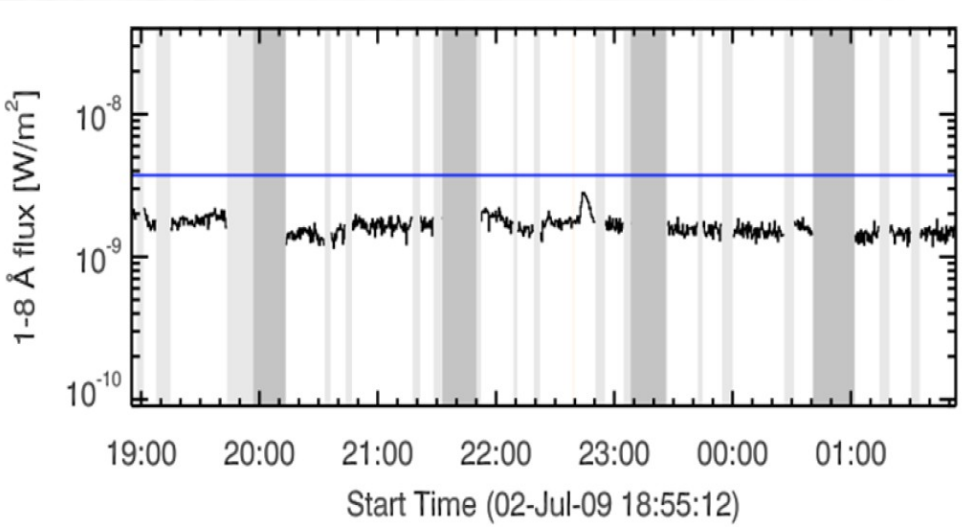

SphinX light curve for quiet Sun. No Active Regions were present on the visible hemisphere during this time interval.

The solar X-ray luminosity

SphinX Measurements During Intervals of Very Low Activity in 2009

Interval	Time Range (Dates are 2009)	T_e (MK)[a]	$\log_{10}$ EM[a] (EM in cm^{-3})	SphinX X-ray (1–8 Å) Flux ($W\ m^{-2}$)[b]	1–15 keV Luminosity ($erg\ s^{-1}$)[b]
1	Feb 20 20:12–Feb 21 05:46	1.73 (.04)	47.81 (.01)	4.91 (−10)	4.63 (22)
2	Feb 21 06:33–Feb 21 15:21	1.81 (.04)	47.72 (.01)	6.62 (−10)	5.10 (22)
3	Mar 2 12:23–Mar 2 17:57	1.89 (.04)	47.61 (.01)	7.70 (−10)	5.15 (22)
4	Mar 3 06:02–Mar 4 00:15	1.88 (.05)	47.62 (.01)	7.60 (−10)	5.15 (22)
5	Mar 4 09:05–Mar 4 17:49	1.84 (.04)	47.68 (.01)	7.21 (−10)	5.22 (22)
6	Mar 4 23:21–Mar 5 11:21	1.79 (.03)	47.78 (.01)	6.48 (−10)	5.33 (22)
7	Mar 5 18:42–Mar 5 20:56	1.80 (.05)	47.69 (.01)	5.90 (−10)	4.66 (22)
8	Mar 11 15:02–Mar 11 20:34	1.79 (.04)	47.83 (.01)	7.35 (−10)	6.03 (22)
9	Apr 12 13:05–Apr 12 17:30	1.74 (.03)	47.93 (.01)	6.68 (−10)	6.16 (22)
10	Apr 13 15:50–Apr 13 20:12	1.72 (.02)	47.95 (.01)	6.38 (−10)	6.11 (22)
11	Apr 14 05:33–Apr 14 11:19	1.74 (.03)	47.92 (.01)	6.66 (−10)	6.10 (22)
12	Apr 19 10:31–Apr 19 14:22	1.85 (.03)	47.75 (.01)	8.64 (−10)	6.16 (22)
13	Apr 19 20:11–Apr 20 05:19	1.92 (.03)	47.64 (.01)	9.85 (−10)	6.20 (22)
14	Apr 20 06:09–Apr 20 12:59	1.88 (.02)	47.73 (.01)	9.76 (−10)	6.56 (22)
15	Jul 18 14:13–Jul 18 16:54	1.72 (.03)	48.01 (.01)	7.28 (−10)	7.01 (22)
16	Jul 18 18:30–Jul 19 02:09	1.73 (.03)	48.00 (.01)	7.59 (−10)	7.09 (22)
17	Jul 22 00:52–Jul 22 04:13	1.75 (.03)	47.97 (.01)	8.17 (−10)	7.31 (22)
18	Aug 12 19:14–Aug 13 09:36	1.74 (.03)	47.98 (.01)	7.79 (−10)	7.11 (22)
19	Aug 19 05:39–Aug 19 20:01	1.72 (.03)	47.96 (.01)	6.34 (−10)	6.14 (22)
20	Aug 19 23:11–Aug 20 10:43	1.68 (.03)	48.05 (.01)	5.99 (−10)	6.44 (22)
21	Aug 20 12:00–Aug 20 18:40	1.87 (.04)	47.75 (.01)	9.89 (−10)	6.81 (22)
22	Sep 11 09:30–Sep 11 22:12	1.79 (.04)	47.83 (.01)	7.64 (−10)	6.16 (22)
23	Sep 11 22:54–Sep 12 12:37	1.70 (.03)	47.99 (.01)	6.05 (−10)	6.12 (22)
24	Sep 13 02:17–Sep 13 07:46	1.69 (.03)	48.01 (.01)	6.10 (−10)	6.27 (22)
25	Sep 13 19:33–Sep 13 21:11	1.68 (.06)	48.02 (.02)	5.80 (−10)	6.13 (22)
26	Sep 14 21:04–Sep 15 07:37	1.79 (.03)	47.84 (.01)	7.79 (−10)	6.28 (22)
27	Sep 16 01:50–Sep 16 07:34	1.71 (.02)	47.99 (.09)	6.53 (−10)	6.48 (22)

The solar X-ray luminosity

Hinode XRT image (Ti-poly filter) taken on 2009 September 15 at 15:47:31 UT. The general corona dominates the total emission in this image, the X-ray bright points accounting for only a small fraction.

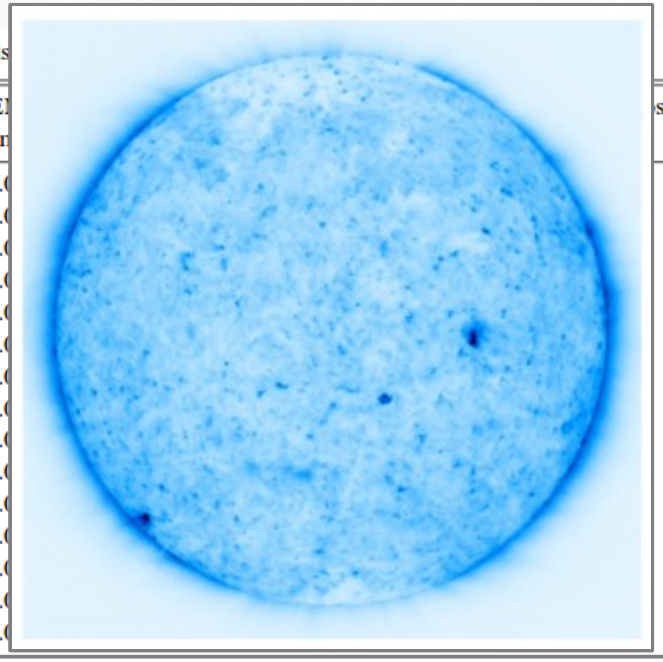

TESIS image in its 171 Å filter taken on September 15 (16:24:27 UT). Solar north is toward the top of both images

22	Sep 11 09:30–Sep 11 22:12	1.79 (.04)	47.83 (.01)	7.64 (−10)	6.16 (22)
23	Sep 11 22:54–Sep 12 12:37	1.70 (.03)	47.99 (.01)	6.05 (−10)	6.12 (22)
24	Sep 13 02:17–Sep 13 07:46	1.69 (.03)	48.01 (.01)	6.10 (−10)	6.27 (22)
26	Sep 14 21:04–Sep 15 07:37	1.79 (.03)	47.84 (.01)	7.79 (−10)	6.28 (22)
27	Sep 16 01:50–Sep 16 07:34	1.71 (.02)	47.99 (.09)	6.53 (−10)	6.48 (22)

Periods of especially low activity

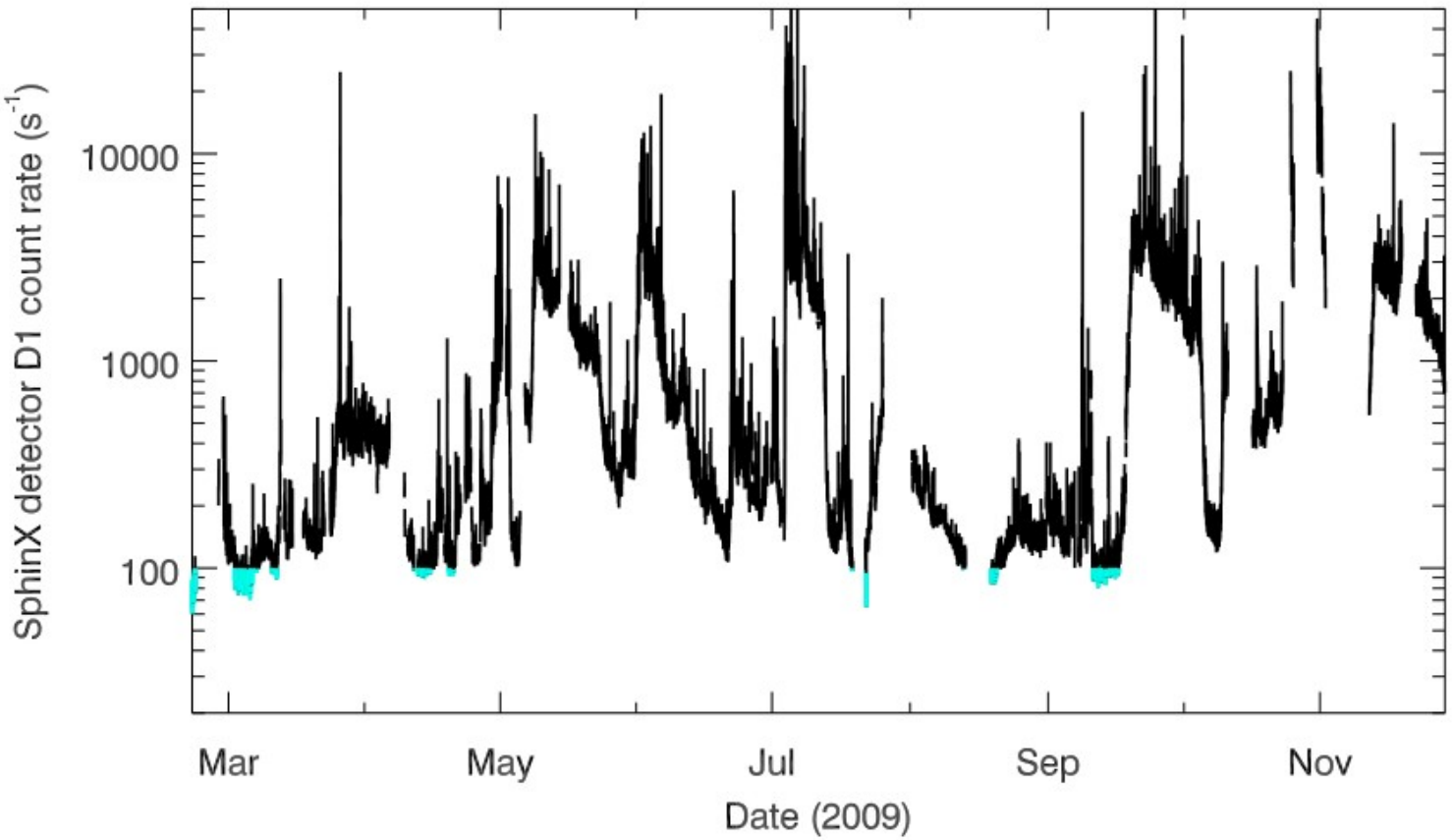

Figure 1. X-ray emission as recorded by the SphinX D1 detector (in counts s^{-1}), from daily averages over the period 2009 February 20–November 28. Portions of the curve marked gray (blue in the online journal) show periods selected for especially low activity. The detector count rates are as observed, i.e., not corrected for the slight variation in the Earth–Sun distance.

Data intervals and sub-interval

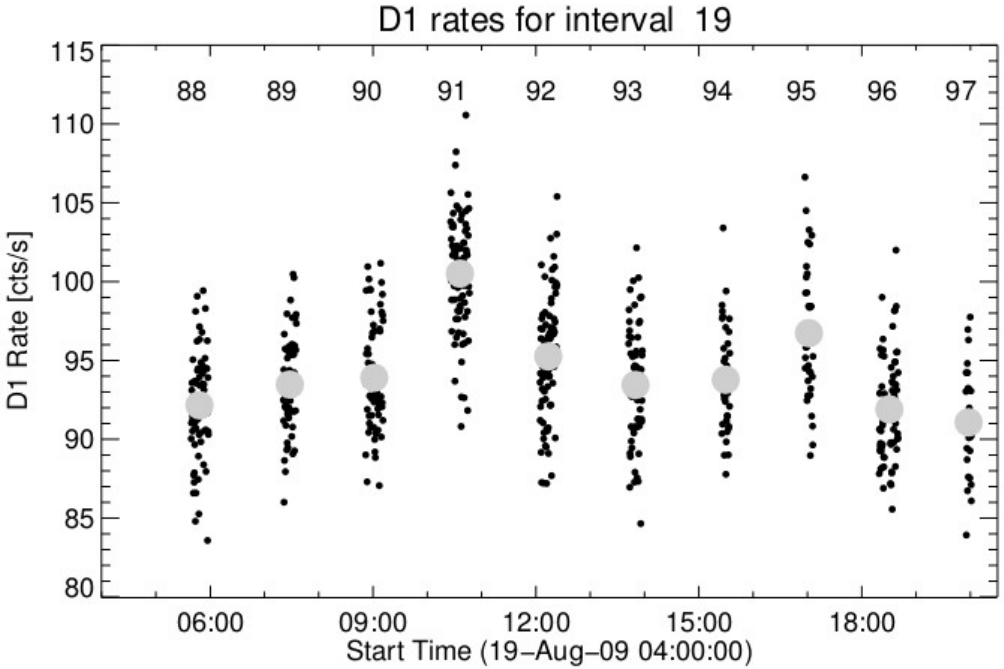

SphinX D1 count rates during interval 19 showing detector D1 counts in sub-intervals 88–97 during this interval. Gray circles are mean count rates for each sub-interval.

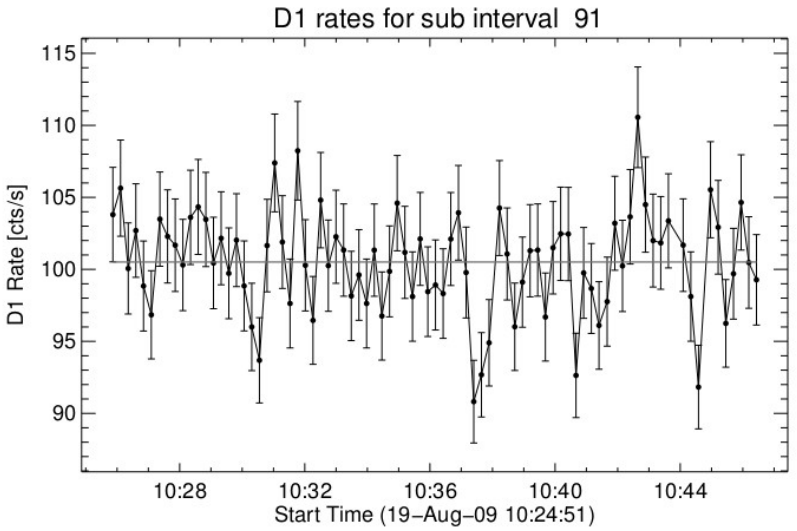

D1 count rates (s^{-1}) for sub-interval 91. Mean count rate (horizontal line) and 1σ statistical uncertainties in the count rates are indicated.

Nanoflares

21-Feb-09 ~11:40

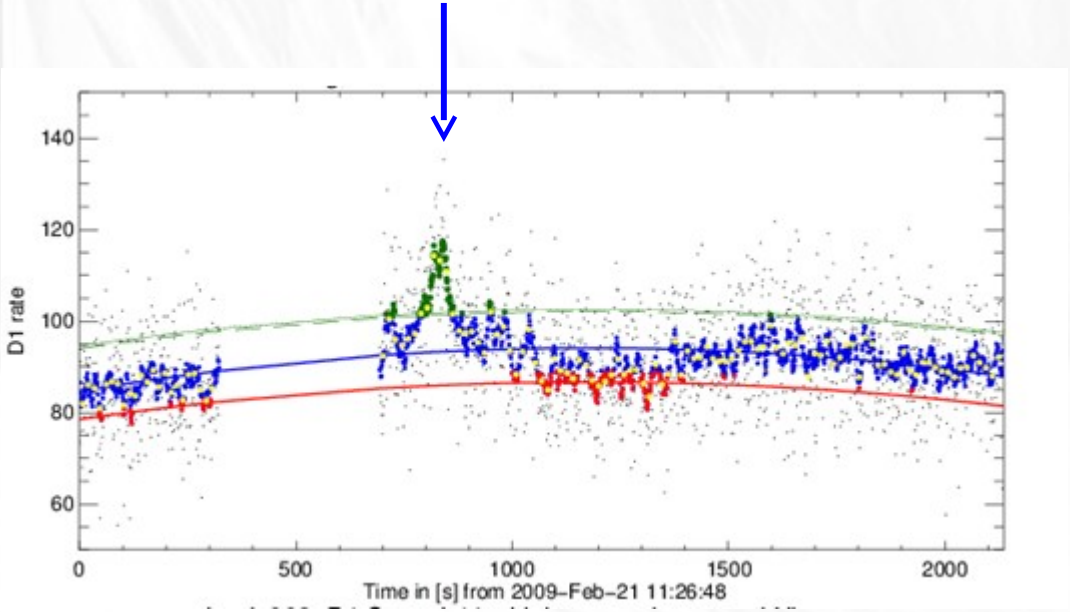

- **14** sub-intervals contain "obvious" events (above 4σ)
- **39** suspected
- **2** long lasting events

UV brightening

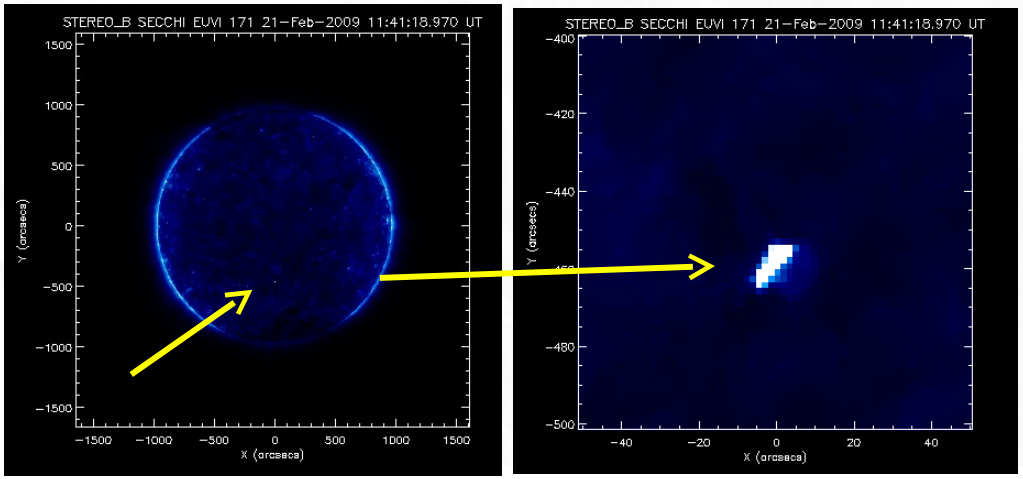

The STEREO-B 171 Å channel image with bright point marked

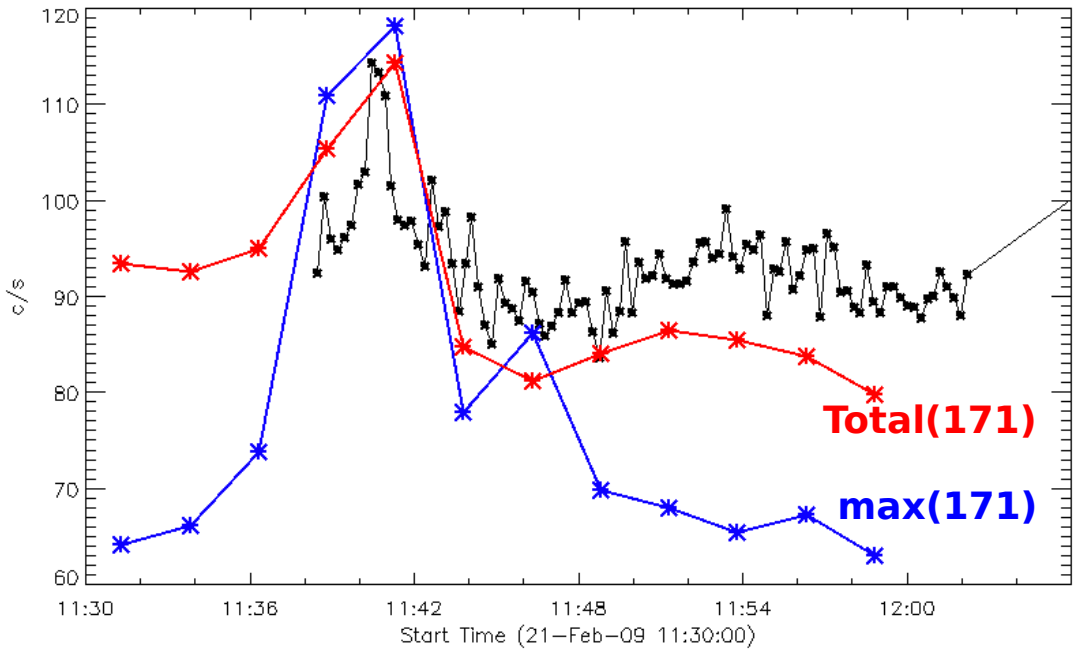

SphinX D1 count rate (s^{-1} : black curve) and total count rate (DN s^{-1}) in STEREO-B 171 Å (Fe IX/Fe X) (red curve) and the maximum count rate in this channel (blue curve) for the brightening seen in the bright point labeled.

Summary

- The SphinX instrument enables for the first time to study the physic of micro- and nanoflares and plasma properties of quiet corona.
- Periods of exceptionally low activity indicating that general coronal temperatures were between 1.7 and 1.9MK, with emission measures between $4x10^{47}cm^{-3}$ and $11x10^{47}cm^{-3}$.
- The SphinX measurement during the period of low activity places the Sun in the 15% of the lowest-activity nearby K and M dwarf stars.
- Need for the instrument similar to SphinX during the next solar minimum.